ACS Partner Journal

CHEM & BIO ENGINEERING

pubs.acs.org/ChemBioEng

Letter

3D-Printable Room Temperature Phosphorescence Polymer Materials with On-Demand Modulation for Modulus Visualization and Anticounterfeiting Applications

Published as part of Chem & Bio Engineering virtual special issue "3D/4D Printing".

Zhen Li, Chuanzhen Zhang, Wenhuan Huang, Chenhui Cui, Kexiang Chen, Zhiyuan He, Ting Xu, Haoqing Teng, Zhishen Ge, Xiaoqing Ming, and Yanfeng Zhang*

Cite This: *Chem Bio Eng.* 2024, 1, 133−140

Read Online

ACCESS | Metrics & More | Article Recommendations | Supporting Information

ABSTRACT: Conventional room temperature phosphorescence (RTP) polymer materials lack a dynamic structural change mechanism for on-demand phosphorescence emission, limiting their application in specific scenarios, such as smart devices. However, the development of RTP polymer materials with an on-demand emission capability is highly attractive yet rather challenging. Herein, we report a novel RTP polymer material that doped purely organic chromophores into a polymer network with numerous free hydroxyl side chains. This unique polymer material can be 3D printed with RTP activated through thermal-triggered nonequilibrium transesterification, where on-demand phosphorescence emission is achieved because of the increased cross-linking degrees such that the thermal motion of chromophores is effectively restricted. As a result, ultralong RTP emission is successfully observed due to enhanced stiffness in the polymer network. Importantly, the modulus changes of the polymer during nonequilibrium transesterification are intuitively visualized based on the intensity of phosphorescence emission. Through liquid crystal display (LCD) 3D printing, complex shaped and multimaterial structured objects are demonstrated, targeting the information encryption of printed objects and on-demand regional emission of multicolored phosphorescence. This study would provide an avenue to control RTP with on-demand emission and contributes to the field of anticounterfeiting and detection applications for intelligent RTP materials.

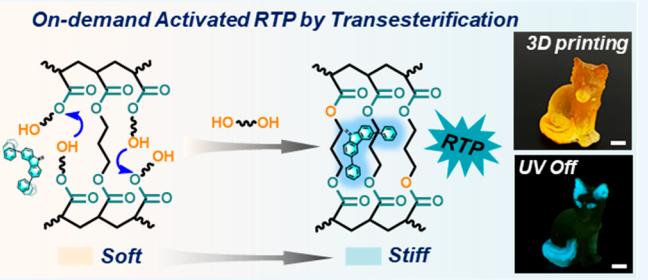

INTRODUCTION

Room temperature phosphorescence (RTP) materials, featured by their long-lived triplet excitons and larger Stokes shift, are increasingly gaining attention in various fields such as information encryption, medical imaging, and optical displays.[1−3] Compared with noble metal based RTP materials, purely organic ones have become attractive alternatives due to their low toxicity, high transparency, and low cost.[4−6] However, the development of long-lived RTP systems remains a significant challenge due to the strong nonradiative decay caused by the quenching of long-lived triplet states by thermal vibrations, oxygen, and other factors and intersystem crossing (ISC) theoretically prohibited.[7,8] In recent years, various strategies have effectively enhanced RTP such as special molecular design and performance enhancement techniques including crystallization,[9,10] host−guest interactions,[11−14] H-aggregation,[15,16] heavy-atom effects,[17−19] and rigid polymer doping.[20−22] Although many long-lived RTP systems have been achieved in the crystalline state, their practical applications are hindered significantly due to poor reproducibility in crystal growth, harsh growth conditions, and lack of flexibility.[23,24]

Polymer based RTP materials, on the other hand, offer broad application prospects due to their better processability, high flexibility, and large-scale production capabilities.[25,26] Importantly, polymer RTP materials provide enormous opportunities for three-dimensional (3D) printing, allowing for the fabrication of complex shapes and structures of solid objects.[27] Traditional RTP polymer materials are usually static and lack the mechanism of dynamic structural change for allowing on-demand phosphorescence emission, thus limiting their broader applications in specific scenarios, such as smart devices. Therefore, developing RTP polymer materials with on-demand emission is highly appealing yet rather challenging.[28−31]

Published: February 23, 2024

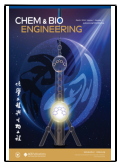

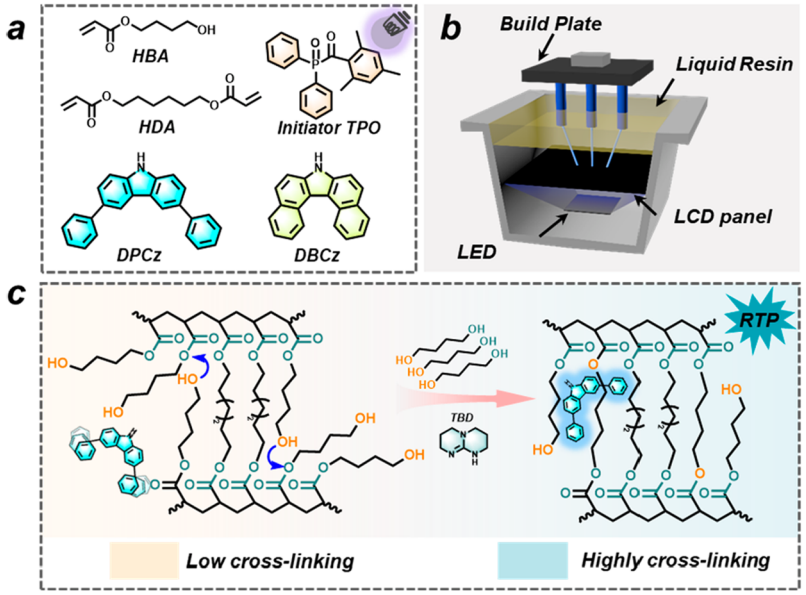

Figure 1. Schematic diagram of chemical structure and transesterification. (a) Chemical structures of monomer, cross-linker, initiator, and chromophores. (b) Schematic illustrations of LCD 3D printing. (c) Polymer network after photopolymerization and the nonequilibrium transesterification.

To enable the development of on-demand RTP polymer materials, inspirations can be drawn from biological organisms that adapt to daily challenges such as support and hunting and alter their structures and modulus on-demand through complex large-scale transport and exchange.[32,33] Inspired from this, we seek to design a polymer system that could be self-stiffened in modulus in a programmable process. The change in modulus of the polymer involves variations in the network's free volume or cross-linking density, and the emission of RTP from chromophores is closely related to the rigid environment of the polymer and can be programmably modulated on demand. For example, the rigid environment of the polymer can constrain the rotational and vibrational thermal motions of organic chromophores, thereby inhibiting the nonradiative decay of triplet excitons and achieving RTP.[34] However, constructing such a self-stiffening polymer system is highly difficult if not impossible.

In recent years, materials with dynamic structures that can rearrange internal topological networks to adapt to the external environment have garnered increasing attention. A key strategy for such adaptive systems involves introducing dynamic covalent chemistry, where specific bonds can undergo reversible breaking and recombination reactions in response to external stimuli.[35−37] Although these materials are dynamic, they manifest a nearly constant modulus, unable to meet our design principle of mechanical stiffening.[38] Recently, Cui et al.[39] proposed a self-stiffening approach based on nonequilibrium transesterification, allowing the initial elastomer to evolve from rubber to plastic with a modulus change of three orders of magnitude, and the stiffening process is also spatially controllable. Based on this strategy, it is envisioned that on-demand RTP emission in polymer materials can be realized.

Herein, we report a novel RTP polymer material with self-stiffening properties by doped purely organic chromophores into a polymer network with numerous free hydroxyl side chains. By utilizing thermally triggered nonequilibrium transesterification, the thermal motion of chromophores is effectively restricted because of the increased cross-linking degree and reduced free volume in the polymer network, resulting in successful RTP emission with on-demand modulation. This unique RTP polymer material based on nonequilibrium transesterification exhibits an ultralong lifetime and allows visualization of the material modulus based on changes in phosphorescence intensity and afterglow. Furthermore, the increased network cross-linking degree induced by transesterification can be spatially controlled by seeding a catalyst in the polymer films, thus selectively activating RTP in specific regions as needed. Moreover, our RTP material can be 3D printed and allows for the fabrication of irregular complex shapes and multimaterial structures. By utilizing on-demand stiffening for encrypting information, the intelligent 3D-printable RTP material demonstrates higher advantages in application fields such as anticounterfeiting and detection.

RESULTS AND DISCUSSION

For the molecular design, the system capable of undergoing a nonequilibrium transesterification consists of an acrylate monomer (4-hydroxybutyl acrylate, HBA), a cross-linker (1,6-hexanediol diacrylate, HDA), a photoinitiator ((2,4,6-trimethylbenzoyldiphenyl)phosphine oxide, TPO), a non-metallic transesterification catalyst (triazobicyclodecene, TBD), and an organic chromophore (3,6-biphenyl-9*H*-carbazole, DPCz and 3,4,5,6-dibenzocarbazol, DBCz), as depicted in the chemical structures shown in Figure 1a. Under 365 nm ultraviolet irradiation, they can also undergo photopolymerization for 3D printing, as illustrated in Figure 1b. The cross-linked polymer network obtained through photopolymerization contains a large number of hydroxyl-terminated side chains. In the presence of the transesterification catalyst TBD, thermally triggered exchange reactions rapidly occur between side-chain hydroxyls and ester bonds. Notably, butanediol molecules generated during the transesterification process can continuously escape from the network at high temperature, thereby persistently driving the transesterification and gradually increasing the degree of cross-linking (Figure 1c).

https://doi.org/10.1021/cbe.3c00128
Chem Bio Eng. 2024, 1, 133−140

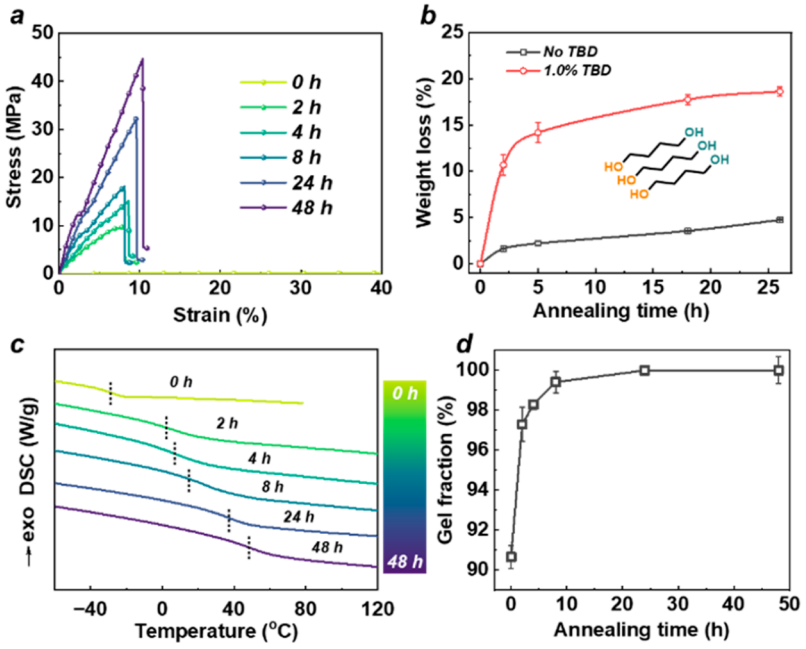

Figure 2. Monitoring the stiffening process. (a) Stress−strain curves, (b) weight loss with and without catalyst (TBD), (c) differential scanning calorimetry (DSC), and (d) gel fraction of HBA-HDA$_{0.2\%}$ after annealing at 150 °C for different time.

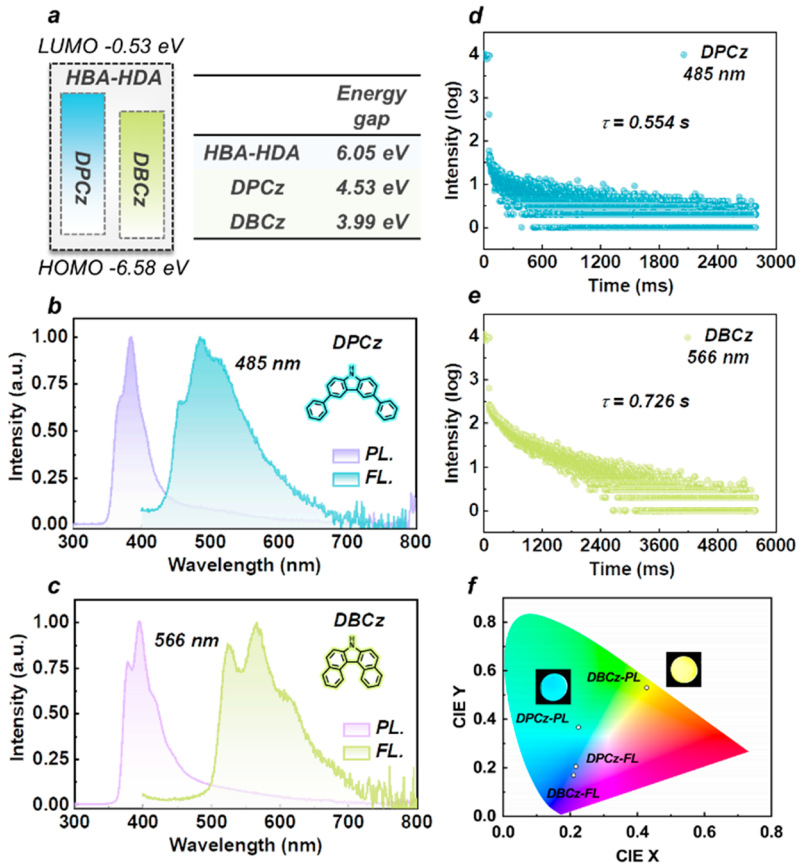

Figure 3. Photophysical properties of DPCz and DBCz doped HBA-HDA$_{0.2\%}$ films. (a) The HOMO and LUMO energy levels of the HBA-HDA (segments) and chromophores. The prompt and delayed phosphorescence spectra of (b) DPCz and (c) DBCz doped HBA-HDA$_{0.2\%}$ films. Lifetime decay curve for the phosphorescence emission peak of (d) HBA-HDA$_{0.2\%}$-DPCz (λ_{em} = 485 nm) and (e) HBA-HDA$_{0.2\%}$-DBCz (λ_{em} = 566 nm) films. (f) CIE coordinate diagram of the films. Annealing conditions: 150 °C for 48 h.

https://doi.org/10.1021/cbe.3c00128
Chem Bio Eng. 2024, 1, 133−140

For 3D printing, the ratio of the monomer (HBA) to cross-linker (HDA) was first screened. By comparing the tensile strength and elongation at break of polymers with different monomer ratios (HBA-HDA$_x$) from uniaxial tensile experiments, the 3D printing ink was determined finally. Within the range 0−3 wt % of the cross-linker HDA, the HBA-HDA$_x$ polymers exhibited moderate elasticity at room temperature. The stress−strain curves show that as the mass ratio of HDA increased, the elongation at break initially increased and then decreased, while the tensile strength exhibited a slow increase followed by a stable trend (Figure S1 and Table S1). Fracture work is another important factor that needs to be considered, which refers to the energy required per unit area for crack propagation under tensile load. It is an important indicator for measuring material resistance to stress failure, representing fracture toughness.[40] The fracture work of HBA-HDA$_x$, calculated from the stress−strain curve, initially increased and then decreased (Figure S2). This is because appropriate cross-linking can enhance the mechanical properties of the material. However, when the degree of cross-linking exceeds a certain threshold, the toughness of material is weakened due to restricted polymer chain movements. Collectively, samples at 0.2 wt % of HDA showed the optimum mechanical performance in terms of tensile strength, elongation at break, and fracture work. Therefore, HBA-HDA$_{0.2\%}$ polymer was selected for further study, unless otherwise specified.

To assess the stiffening behavior of the HBA-HDA$_{0.2\%}$ material, we preliminarily monitored the transesterification-induced cross-linking reaction process. After the sample was annealed at 150 °C for 5 h, the tensile strength increased from 0.6 to 15 MPa due to transesterification (Figure S3). In comparison, samples without the transesterification catalyst TBD were treated under the same conditions, and no significant stiffening was observed, indicating the transesterification-induced stiffening mechanism.

Moreover, the stiffening process was dependent on the annealing time at 150 °C. With increasing annealing time (0−48 h), the uniaxial tensile modulus of HBA-HDA$_{0.2\%}$ gradually increased from 0.5 to 617 MPa, and the tensile strength increased from 0.6 to 44.7 MPa, while the elongation at break significantly decreased from 645% to 11% (Figure 2a and Table S2). This significant change in mechanical properties is attributed to the increased cross-linking density induced by nonequilibrium transesterification. To confirm the occurrence of transesterification, weight of the sample was monitored. Results show that due to the evaporation of the byproduct butanediol, the stiffening process was always accompanied by a decrease in sample weight, whereas the mass of samples without the transesterification catalyst TBD remained almost unchanged (Figure 2b). Attenuated total reflection Fourier transform infrared spectroscopy (ATR-FTIR) showed that the vibrational intensity of −OH (~3420 cm^{-1}) and C−H (~2919 and 2852 cm^{-1}) significantly decreased, also confirming the removal of butanediol (Figure S4). During the annealing process, the glass transition temperature (T_g) presented a dramatic elevation from −28 to 50 °C due to an increased degree of cross-linking, indicating a transition from rubbery to glassy state well consistent with the stiffening phenomenon (Figure 2c). In addition, the gel fraction of the polymer, determined by mass changes after dissolution equilibrium, increased from 90% to 99% with extended annealing time, confirming that stiffening is accompanied by an increase in the polymer's cross-linking density (Figure 2d). The higher cross-linking degree also results in a lower swelling ratio (Figure S5).

The highly cross-linked and rigid polymer environment obtained after nonequilibrium transesterification effectively restricts the thermal motion of organic chromophores, suppressing the nonradiative decay of triplet excitons, thus achieving RTP emission. Therefore, it is essential to first examine the frontier orbitals and energy levels of HBA-HDA and the chromophores (DPCz and DBCz). As shown in Table S3 and Figure 3a, the energy gap of the HBA-HDA polymer matrix (6.05 eV) is sufficiently large to cover the energy gaps of both chromophores (DPCz and DBCz), avoiding electron transfer between the polymer matrix and the fluorophores.[41] These results indicate that the HBA-HDA polymer matrix is an ideal carrier for preparing a purely organic RTP polymer system.

To further validate this, the organic chromophores DPCz and DBCz were simply doped into the monomer HBA, cross-linker HDA, and catalyst TBD for photopolymerization. Surprisingly, after annealing for 48 h via nonequilibrium transesterification, a dense three-dimensional cross-linked network could effectively constrain the thermal motion, including rotation and vibration of the chromophores, successfully establishing a purely organic RTP polymer system. At room temperature, after removing 365 nm UV irradiation, both HBA-HDA$_{0.2\%}$-DPCz and HBA-HDA$_{0.2\%}$-DBCz exhibited intense afterglow (blue and yellow) visible to the naked eye, with ultralong emission lasting for 10 and 6 s, respectively (Figure S6). The lack of sharp and strong peaks in the X-ray diffraction (XRD) patterns indicates that HBA-HDA$_{0.2\%}$ doped with DPCz and DBCz exhibited an amorphous phase (Figure S7).

To investigate the impact of the chromophores (DPCz and DBCz) on transesterification, samples doped with DPCz and DBCz, denoted as HBA-HDA$_{0.2\%}$-DPCz and HBA-HDA$_{0.2\%}$-DBCz, exhibited mechanical properties similar to those of HBA-HDA$_{0.2\%}$ after annealing at 150 °C (Figure S8). Their tensile strengths were 16 and 17 MPa, respectively, indicating comparable levels of stiffening induced by transesterification. Furthermore, both DPCz and DBCz-doped samples of HBA-HDA$_{0.2\%}$ displayed a significant decrease in vibrational intensity for −OH (~3420 cm^{-1}) and C−H (~2919 and 2852 cm^{-1}), again confirming the removal of butanediol (Figure S9). The stiffening process also accompanied a change in T_g, with HBA-HDA$_{0.2\%}$-DPCz/DBCz samples showing an increase in T_g from −28 and −30 °C to 49 and 52 °C, respectively, after 48 h of heat treatment (Figure S10). In comparison to those of the purely HBA-HDA$_{0.2\%}$ sample, the T_g values were nearly identical. These experiments conclusively demonstrate that the introduction of chromophores has no significant impact on the nonequilibrium transesterification in the system because of their extremely small doping amounts.

Furthermore, to examine the source of RTP in HBA-HDA$_{0.2\%}$-DPCz/DBCz, steady-state and transient spectra were recorded. All RTP polymers exhibited dual-emission features, as shown in Figure 3b,c. For example, the emission at 485 nm from HBA-HDA$_{0.2\%}$-DPCz lasted for 0.554 s (Figure 3d), with a lifetime of 8.20 at 384 nm (Figure S11). It is reported that dual-emission features can be attributed to the fluorescence and phosphorescence of the chromophores doped in the polymer.[42] Phosphorescence spectra measured in dilute solutions (DPCz and DBCz) at a low temperature (77 K) further supported this result, exhibiting the same electronic structure as the polymer at room temperature (Figure S12). Simultaneously, a long-lived yellow RTP emission (τ = 0.726 s) was successfully obtained

https://doi.org/10.1021/cbe.3c00128
Chem Bio Eng. 2024, 1, 133−140

from HBA-HDA$_{0.2\%}$-DBCz (Figure 3e). The Commission Internationale de l'Eclairage (CIE) coordinate diagrams were calculated for their phosphorescence spectra using spectrograph software (Figure 3f), resulting in coordinates (0.22, 0.37) for DPCz and (0.43, 0.53) for DBCz, respectively. The long lifetime of this purely organic RTP polymer material primarily originated from the rigid environment in the cross-linked polymer matrix.

Annealing time has great influence on the reaction degree of transesterification, thus leading to different degrees of cross-linking and rigidity. The phosphorescence emission of the chromophores is closely related to the rigid structure of the polymer matrix. It is reasoned that the soft-to-stiff transition of polymers can be visualized through the RTP emission intensity of the chromophores. To verify this hypothesis, HBA-HDA$_{0.2\%}$-DPCz samples were heat-treated for various durations (0−48 h), and their phosphorescence emissions were recorded. As shown in Figure 4a, with increasing heat treatment time, phosphorescence gradually appeared, and polymer films annealed for different times exhibited distinct phosphorescence intensity and afterglow time. Phosphorescent intensity and afterglow time increased with annealing time (Figure 4b). Additionally, after annealing for more than 8 h, the phosphorescent intensity and afterglow time remained relatively constant. Calculations showed that after 8 h of annealing, the gel fraction of the material was 99%, indicating that the polymer matrix was in a highly cross-linked state. Moreover, as shown in Figure 4c polymers with gradient moduli obtained from different degrees of transesterification also exhibit gradient variations in phosphorescence intensity and afterglow, suggesting that the cross-linking degree and modulus of polymeric materials can be successfully visualized in a nondestructive manner with a shape-independent measurement. To further demonstrate the universality of this strategy, as shown in Figures S13 and S14, the same annealing conditions were applied to HBA-HDA$_{0.2\%}$-DBCz. With an increasing annealing time, HBA-HDA$_{0.2\%}$-DBCz exhibited a similar trend of changes in phosphorescence intensity and afterglow time. These findings indicate that the RTP emission intensity of the chromophores depends on the cross-linking density of polymer matrix, making this strategy promising for the modulus visualization of polymer materials.

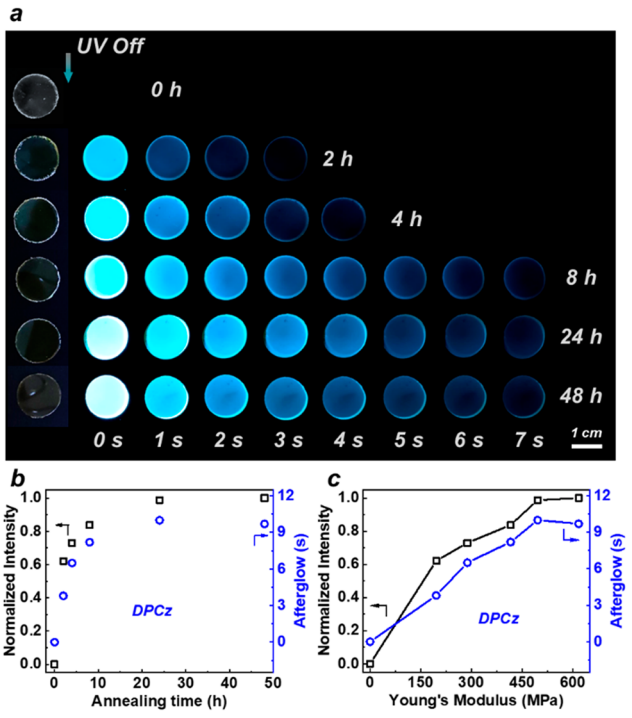

Figure 4. Photophysical properties of HBA-HDA$_{0.2\%}$-DPCz films after nonequilibrium transesterification for different times. (a) Phosphorescence photographs of HBA-HDA$_{0.2\%}$-DPCz films (Φ = 15 mm) after annealing at 150 °C for different times at room temperature. Phosphorescence intensity and afterglow of HBA-HDA$_{0.2\%}$-DPCz films for (b) different annealing times and (c) different Young's modulus.

The specific process of increasing network cross-linking density through transesterification can be selectively controlled by spatially seeding a catalyst in the sample. As illustrated in Figure 5a, a solution of transesterification catalyst TBD was selectively dripped onto the surface of the prepared HBA-HDA$_{0.2\%}$-DPCz/DBCz sample without the transesterification catalyst. After annealing for 24 h, the region where the transesterification catalyst TBD was seeded exhibited an increased degree of localized cross-linking, suppressing the nonradiative transitions of the chromophores DPCz and DBCz, resulting in patterned RTP materials. As shown in Figure 5b,c, various patterned phosphorescence emissions were achieved through catalyst seeding, successfully obtaining blue and yellow RTP with patterns such as "Ester", "Carbazole", "XJTU", and "3D" (Supporting Movies S1−S6). Their afterglow spectra were recorded (Figure S15), showing that transesterification catalyst TBD incorporated in a way (mixing and dripping) that it did not affect the electronic structure of the chromophores. Using heat to activate RTP, particularly in polymeric systems, is rarely explored,[43−45] and thanks to the spatially regionalized control

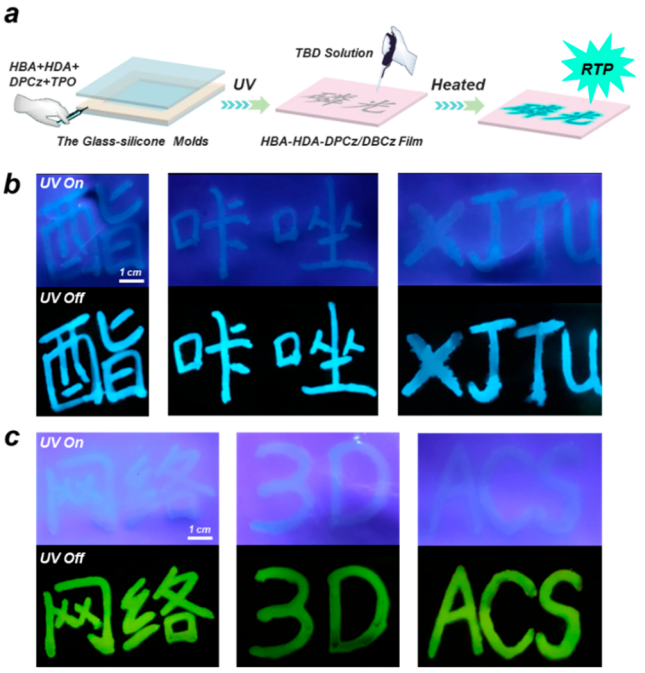

Figure 5. Patterned phosphorescence by nonequilibrium transesterification. (a) Process of obtaining regionalized phosphorescence. Photographs of (b) HBA-HDA$_{0.2\%}$-DPCz and (c) HBA-HDA$_{0.2\%}$-DBCz films with writing by TBD solution before and after turning off the UV irradiation at room temperature (annealing conditions: 150 °C for 24 h).

https://doi.org/10.1021/cbe.3c00128
Chem Bio Eng. 2024, 1, 133−140

property of on-demand hardening, this is a novel RTP thermally activated patterning strategy enhancing the advantages of smart RTP materials in application fields such as anticounterfeiting, sensing, and detection.

3D-printable RTP materials are of interest due to the growing demand for irregular shapes and multimaterial structures.[46,47] 3D printing, also known as additive manufacturing (AM), has become an advanced and versatile technology for rapid on-demand fabrication of solid objects.[48] Unlike traditional manufacturing processes, additive manufacturing tools can produce arbitrarily complex shapes characterized by layered and intricate structures, featuring hollow features and multimaterial structures. In contrast to traditional 3D printing, this 3D printing ink is doped with chromophores, enabling the localized activation of phosphorescence after thermally triggered transesterification, achieving a diversity of shapes in smart RTP materials. As shown in Figure 6, a series of samples with complex

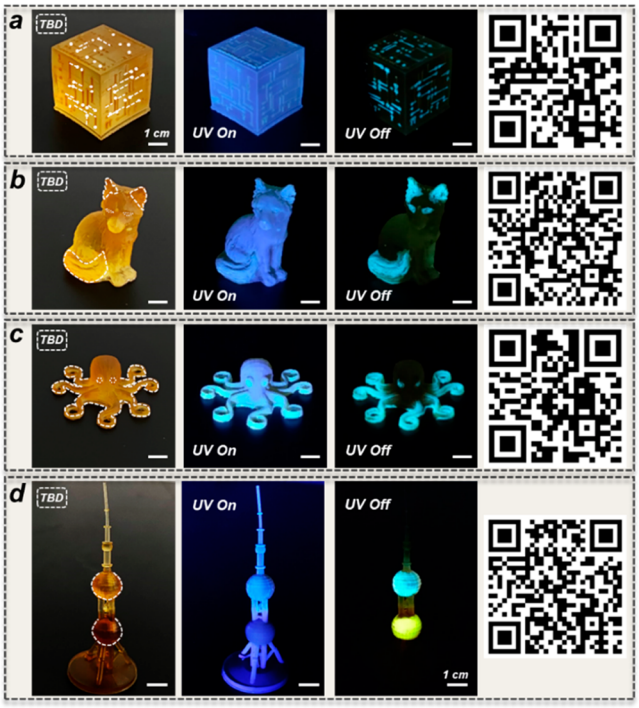

Figure 6. Spatial regionalization activates phosphorescence of 3D printing materials. Photographs and luminescence photographs of 3D printing (a) cube, (b) fox, (c) octopus, and (d) Oriental Pearl tower under and after UV irradiation following nonequilibrium transesterification (annealing conditions: 150 °C for 24 h). Scan the QR code to watch the movies.

three-dimensional structures were obtained using liquid crystal display (LCD) 3D printing. These samples exhibited elasticity at room temperature and could withstand deformations. By controlling the seeding position of the transesterification catalyst TBD in the 3D-printed samples, continuous nonequilibrium transesterification was triggered through heat treatment. After annealing for 24 h, the localized cross-linking density increased in the region where the catalyst was seeded, resulting in material stiffening and activation of phosphorescent emission. In Figure 6a, a cube with pattern information was printed using 3D printing, and the catalyst TBD was seeded in part of the routes. After heat treatment, the routes seeded with TBD exhibited a distinct blue RTP emission, while the unstiffened routes showed no RTP emission (Supporting Movie S7), providing a new method for visualizing anticounterfeiting encryption of 3D printed materials. Similarly, different examples of 3D-printed shapes with regionally activated blue phosphorescence emission such as "tail of fox" and "tentacles of octopus" (Supporting Movies S8 and S9), as well as yellow RTP emission like "feeler" were obtained through spatially activated RTP (Figure 6b,c and Figure S16). Notably, due to the layered characteristics of 3D printing, multimaterial structures can be prepared in 3D-printed samples, enabling the realization of regionally dual-color phosphorescent emission resembling the Oriental Pearl tower (Figure 6d and Supporting Movie S10). 3D printing offers diversity in the shape and structure of smart RTP materials, showcasing significant potential for practical applications of 3D-printable intelligent RTP materials.

CONCLUSION

In summary, we have successfully developed a purely organic RTP polymer material that can be selectively activated on demand by incorporating chromophores into the polymer. This material is amenable to 3D printing and can achieve on-demand, ultralong multicolor RTP emission through transesterification reactions. Within a certain range, the phosphorescence intensity and afterglow time are positively correlated with the material's modulus, allowing for the intuitive detection of modulus changes during nonequilibrium transesterification. Additionally, various patterned RTP materials can be obtained by selectively seeding transesterification catalysts on the polymer films, as needed. Combining with 3D printing, we demonstrate information encryption visualization in 3D printed objects with complex shapes and multimaterial structures and on-demand regionally emitted multicolor RTP. This work provides a strategy for the on-demand modulation of smart RTP materials in the fields of anticounterfeiting encryption and modulus detection.

ASSOCIATED CONTENT

Supporting Information

The Supporting Information is available free of charge at https://pubs.acs.org/doi/10.1021/cbe.3c00128.

Materials, characterization methods, synthesis; figures of stress−strain curves and tests, breaking strength, elongation at break, and fracture work, FTIR spectra, swelling ratio, HOMO and LUMO energy levels, luminescence photographs, XRD patterns, DSC profiles, transient decay curves, phosphorescence spectra, phosphorescence photographs, phosphorescence intensity and afterglow, delayed spectra, optical and luminescence photographs; tables of breaking strength and elongation at break and of Young's modulus (PDF)

Supporting Movie S1. DPCz-doped HBA-HDA$_{0.2\%}$ films show patterned phosphorescence ("Ester") (MP4)

Supporting Movie S2. DPCz-doped HBA-HDA$_{0.2\%}$ films show patterned phosphorescence ("Carbazole") (MP4)

Supporting Movie S3. DPCz-doped HBA-HDA$_{0.2\%}$ films show patterned phosphorescence ("XJTU") (MP4)

Supporting Movie S4. DBCz-doped HBA-HDA$_{0.2\%}$ films show patterned phosphorescence ("Network") (MP4)

Supporting Movie S5. DBCz-doped HBA-HDA$_{0.2\%}$ films show patterned phosphorescence ("3D") (MP4)

Supporting Movie S6. DBCz-doped HBA-HDA$_{0.2\%}$ films show patterned phosphorescence ("ACS") (MP4)

https://doi.org/10.1021/cbe.3c00128
Chem Bio Eng. 2024, 1, 133−140

Supporting Movie S7. DPCz-doped 3D printing show patterned phosphorescence (MP4)

Supporting Movie S8. DPCz-doped 3D printing show patterned phosphorescence ("Fox") (MP4)

Supporting Movie S9. DPCz-doped 3D printing show patterned phosphorescence Octopus (MP4)

Supporting Movie S10. DPCz and DBCz-doped 3D printing show patterned phosphorescence (MP4)

AUTHOR INFORMATION

Corresponding Author

Yanfeng Zhang − *School of Chemistry, Engineering Research Center of Energy Storage Materials and Devices, Ministry of Education, Xi'an Jiaotong University, Xi'an, Shaanxi 710049, China*; orcid.org/0000-0003-4711-8690; Email: yanfengzhang@mail.xjtu.edu.cn

Authors

Zhen Li − *School of Chemistry, Engineering Research Center of Energy Storage Materials and Devices, Ministry of Education, Xi'an Jiaotong University, Xi'an, Shaanxi 710049, China*

Chuanzhen Zhang − *School of Chemistry, Engineering Research Center of Energy Storage Materials and Devices, Ministry of Education, Xi'an Jiaotong University, Xi'an, Shaanxi 710049, China*

Wenhuan Huang − *Hefei National Research Center for Physical Sciences at the Microscale, University of Science and Technology of China, Hefei, Anhui 230026, China*

Chenhui Cui − *School of Chemistry, Engineering Research Center of Energy Storage Materials and Devices, Ministry of Education, Xi'an Jiaotong University, Xi'an, Shaanxi 710049, China*

Kexiang Chen − *School of Chemistry, Engineering Research Center of Energy Storage Materials and Devices, Ministry of Education, Xi'an Jiaotong University, Xi'an, Shaanxi 710049, China*

Zhiyuan He − *School of Chemistry, Engineering Research Center of Energy Storage Materials and Devices, Ministry of Education, Xi'an Jiaotong University, Xi'an, Shaanxi 710049, China*

Ting Xu − *School of Chemistry, Engineering Research Center of Energy Storage Materials and Devices, Ministry of Education, Xi'an Jiaotong University, Xi'an, Shaanxi 710049, China*

Haoqing Teng − *School of Chemistry, Engineering Research Center of Energy Storage Materials and Devices, Ministry of Education, Xi'an Jiaotong University, Xi'an, Shaanxi 710049, China*

Zhishen Ge − *School of Chemistry, Engineering Research Center of Energy Storage Materials and Devices, Ministry of Education, Xi'an Jiaotong University, Xi'an, Shaanxi 710049, China*

Xiaoqing Ming − *School of Chemistry, Engineering Research Center of Energy Storage Materials and Devices, Ministry of Education, Xi'an Jiaotong University, Xi'an, Shaanxi 710049, China*; orcid.org/0000-0002-8290-5094

Complete contact information is available at: https://pubs.acs.org/10.1021/cbe.3c00128

Author Contributions

Zhen Li and Chuanzhen Zhang contributed equally to this paper. All authors have given approval to the final version of the manuscript.

Notes

The authors declare no competing financial interest.

ACKNOWLEDGMENTS

This work was supported by the National Key R&D Program of China (2019YFA0706801), the National Natural Science Foundation of China (NSFC 52173079), the Fundamental Research Funds for the Central Universities (xtr052023001, xzy012023037), and the Shaanxi Provincial Natural Science Basic Research Program-Shaanxi Coal Joint Fund (2021JLM-40). The authors thank the Instrument Analysis Center of Xi'an Jiaotong University for the assistance with the steady and delayed spectra, XRD, DSC analysis, and Analytical Test Platform of School of Chemistry with ATR-FTIR analysis.

REFERENCES

(1) Gao, Q.; Shi, M.; Lü, Z.; Zhao, Q.; Chen, G.; Bian, J.; Qi, H.; Ren, J.; Lü, B.; Peng, F. Large-Scale Preparation for Multicolor Stimulus-Responsive Room-Temperature Phosphorescence Paper via Cellulose Heterogeneous Reaction. *Adv. Mater.* **2023**, *35* (47), 2305126.

(2) Wang, Y.; Yang, J.; Fang, M.; Yu, Y.; Zou, B.; Wang, L.; Tian, Y.; Cheng, J.; Tang, B. Z.; Li, Z. Förster Resonance Energy Transfer: An Efficient Way to Develop Stimulus-Responsive Room-Temperature Phosphorescence Materials and Their Applications. *Matter* **2020**, *3* (2), 449−463.

(3) Lei, Y.; Dai, W.; Li, G.; Zhang, Y.; Huang, X.; Cai, Z.; Dong, Y. Stimulus-Responsive Organic Phosphorescence Materials Based on Small Molecular Host−Guest Doped Systems. *J. Phys. Chem. Lett.* **2023**, *14* (7), 1794−1807.

(4) Gan, N.; Shi, H.; An, Z.; Huang, W. Recent Advances in Polymer-Based Metal-Free Room-Temperature Phosphorescent Materials. *Adv. Funct. Mater.* **2018**, *28* (51), 1802657.

(5) Zhang, T.; Ma, X.; Wu, H.; Zhu, L.; Zhao, Y.; Tian, H. Molecular Engineering for Metal-Free Amorphous Materials with Room-Temperature Phosphorescence. *Angew. Chem., Int. Ed.* **2020**, *59* (28), 11206−11216.

(6) Gong, Y.; Yang, J.; Fang, M.; Li, Z. Room-temperature phosphorescence from metal-free polymer-based materials. *Cell Rep. Phys. Sci.* **2022**, *3* (2), 100663.

(7) Shi, H.; Yao, W.; Ye, W.; Ma, H.; Huang, W.; An, Z. Ultralong Organic Phosphorescence: From Material Design to Applications. *Accounts Chem. Res.* **2022**, *55* (23), 3445−3459.

(8) Ma, L.; Ma, X. Recent advances in room-temperature phosphorescent materials by manipulating intermolecular interactions. *Sci. China Chem.* **2023**, *66* (2), 304−314.

(9) Yuan, W. Z.; Shen, X. Y.; Zhao, H.; Lam, J. W. Y.; Tang, L.; Lu, P.; Wang, C.; Liu, Y.; Wang, Z.; Zheng, Q.; Sun, J. Z.; Ma, Y.; Tang, B. Z. Crystallization-Induced Phosphorescence of Pure Organic Luminogens at Room Temperature. *J. Phys. Chem. C* **2010**, *114* (13), 6090−6099.

(10) Bolton, O.; Lee, K.; Kim, H.-J.; Lin, K. Y.; Kim, J. Activating Efficient Phosphorescence from Purely Organic Materials by Crystal Design. *Nat. Chem.* **2011**, *3* (3), 205−210.

(11) Guo, S.; Dai, W.; Chen, X.; Lei, Y.; Shi, J.; Tong, B.; Cai, Z.; Dong, Y. Recent Progress in Pure Organic Room Temperature Phosphorescence of Small Molecular Host−Guest Systems. *ACS Materials Lett.* **2021**, *3* (4), 379−397.

(12) Chen, B.; Huang, W.; Nie, X.; Liao, F.; Miao, H.; Zhang, X.; Zhang, G. An Organic Host−Guest System Producing Room-Temperature Phosphorescence at the Parts-Per-Billion Level. *Angew. Chem., Int. Ed.* **2021**, *60* (31), 16970−16973.

(13) Ren, Y.; Dai, W.; Guo, S.; Dong, L.; Huang, S.; Shi, J.; Tong, B.; Hao, N.; Li, L.; Cai, Z.; Dong, Y. Clusterization-Triggered Color-Tunable Room-Temperature Phosphorescence from 1,4-Dihydropyridine-Based Polymers. *J. Am. Chem. Soc.* **2022**, *144* (3), 1361−1369.

(14) Yan, X.; Peng, H.; Xiang, Y.; Wang, J.; Yu, L.; Tao, Y.; Li, H.; Huang, W.; Chen, R. Recent Advances on Host-Guest Material Systems

toward Organic Room Temperature Phosphorescence. *Small* **2022**, *18* (1), 2104073.
(15) Miao, Y.; Liu, S.; Ma, L.; Yang, W.; Li, J.; Lv, J. Ultralong and Color-Tunable Room-Temperature Phosphorescence Based on Commercial Melamine for Anticounterfeiting and Information Recognition. *Anal. Chem.* **2021**, *93* (8), 4075−4083.
(16) Yuan, J.; Wang, S.; Ji, Y.; Chen, R.; Zhu, Q.; Wang, Y.; Zheng, C.; Tao, Y.; Fan, Q.; Huang, W. Invoking Ultralong Room Temperature Phosphorescence of Purely Organic Compounds through H-aggregation Engineering. *Mater. Horiz.* **2019**, *6* (6), 1259−1264.
(17) Yan, Z.-A.; Ma, X. External Heavy-Atom Activated Phosphorescence of Organic Luminophores in a Rigid Fluid Matrix. *ACS Materials Lett.* **2022**, *4* (12), 2555−2561.
(18) Zhang, G.; Chen, J.; Payne, S. J.; Kooi, S. E.; Demas, J. N.; Fraser, C. L. Multi-Emissive Difluoroboron Dibenzoylmethane Polylactide Exhibiting Intense Fluorescence and Oxygen-Sensitive Room-Temperature Phosphorescence. *J. Am. Chem. Soc.* **2007**, *129* (29), 8942−8943.
(19) Zhang, Y.; Chen, X.; Xu, J.; Zhang, Q.; Gao, L.; Wang, Z.; Qu, L.; Wang, K.; Li, Y.; Cai, Z.; Zhao, Y.; Yang, C. Cross-Linked Polyphosphazene Nanospheres Boosting Long-Lived Organic Room-Temperature Phosphorescence. *J. Am. Chem. Soc.* **2022**, *144* (13), 6107−6117.
(20) Wu, H.; Wang, D.; Zhao, Z.; Wang, D.; Xiong, Y.; Tang, B. Z. Tailoring Noncovalent Interactions to Activate Persistent Room-Temperature Phosphorescence from Doped Polyacrylonitrile Films. *Adv. Funct. Mater.* **2021**, *31* (32), 2101656.
(21) Wu, B.; Guo, N.; Xu, X.; Xing, Y.; Shi, K.; Fang, W.; Wang, G. Ultralong and High-Efficiency Room Temperature Phosphorescence of Organic-Phosphors-Doped Polymer Films Enhanced by 3D Network. *Adv. Opt. Mater.* **2020**, *8* (22), 2001192.
(22) Zhang, Y.; Gao, L.; Zheng, X.; Wang, Z.; Yang, C.; Tang, H.; Qu, L.; Li, Y.; Zhao, Y. Ultraviolet Irradiation-responsive Dynamic Ultralong Organic Phosphorescence in Polymeric Systems. *Nat. Commun.* **2021**, *12* (1), 2297.
(23) Zhang, X.; Qian, C.; Ma, Z.; Fu, X.; Li, Z.; Jin, H.; Chen, M.; Jiang, H.; Ma, Z. A Class of Organic Units Featuring Matrix-Controlled Color-Tunable Ultralong Organic Room Temperature Phosphorescence. *Adv. Sci.* **2023**, *10* (3), 2206482.
(24) Gu, L.; Wu, H.; Ma, H.; Ye, W.; Jia, W.; Wang, H.; Chen, H.; Zhang, N.; Wang, D.; Qian, C.; An, Z.; Huang, W.; Zhao, Y. Color-tunable Ultralong Organic Room Temperature Phosphorescence from a Multicomponent Copolymer. *Nat. Commun.* **2020**, *11* (1), 944.
(25) Guo, J.; Yang, C.; Zhao, Y. Long-Lived Organic Room-Temperature Phosphorescence from Amorphous Polymer Systems. *Accounts Chem. Res.* **2022**, *55* (8), 1160−1170.
(26) Li, C.; Guo, F.; Zhu, Y.; Zhou, Q.; Chen, Q.; Wang, Y.; Huang, J.; Qu, L.; Yang, C. Ink-Free Screen Printing in Water Environment-Based Slightly Cross-Linked Polymer Phosphorescence Systems. *Macromolecules* **2023**, *56* (24), 10028−10036.
(27) Roppolo, I.; Caprioli, M.; Pirri, C. F.; Magdassi, S. 3D Printing of Self-Healing Materials. *Adv. Mater.* **2023**, DOI: 10.1002/adma.202305537.
(28) Zhou, Q.; Yang, C.; Zhao, Y. Dynamic Organic Room-temperature Phosphorescent Systems. *Chem.* **2023**, *9* (9), 2446−2480.
(29) Gu, F.; Ma, X. Stimuli-Responsive Polymers with Room-Temperature Phosphorescence. *Chem.—Eur. J.* **2022**, *28* (15), No. e202104131.
(30) Gu, L.; Wang, X.; Singh, M.; Shi, H.; Ma, H.; An, Z.; Huang, W. Organic Room-Temperature Phosphorescent Materials: From Static to Dynamic. *J. Phys. Chem. Lett.* **2020**, *11* (15), 6191−6200.
(31) Yang, J.; Fang, M.; Li, Z. Stimulus-Responsive Room Temperature Phosphorescence Materials: Internal Mechanism, Design Strategy, and Potential Application. *Accounts Chem. Res.* **2021**, *2* (8), 644−654.
(32) Wojtecki, R. J.; Meador, M. A.; Rowan, S. J. Using the Dynamic Bond to Access Macroscopically Responsive Structurally Dynamic Polymers. *Nat. Mater.* **2011**, *10* (1), 14−27.
(33) Shi, X.; Zhang, K.; Chen, J.; Qian, H.; Huang, Y.; Jiang, B. Octopi Tentacles-Inspired Architecture Enables Self-Healing Conductive Rapid-Photo-Responsive Materials for Soft Multifunctional Actuators. *Adv. Funct. Mater.* **2024**, *34* (6), 2311567.
(34) Sun, Z.; Deng, H.; Mao, Z.; Li, Z.; Nie, K.; Fu, K.; Chen, J.; Zhao, J.; Zhu, P.; Chi, Z.; Sun, R. Shape-Memorable, Self-Healable, Recyclable, and Full-Color Emissive Ultralong Organic Phosphorescence Vitrimers with Exchangeable Covalent Bonds. *Adv. Opt. Mater.* **2022**, *10* (23), 2201558.
(35) Miao, W.; Yang, B.; Jin, B.; Ni, C.; Feng, H.; Xue, Y.; Zheng, N.; Zhao, Q.; Shen, Y.; Xie, T. An Orthogonal Dynamic Covalent Polymer Network with Distinctive Topology Transformations for Shape- and Molecular Architecture Reconfiguration. *Angew. Chem., Int. Ed.* **2022**, *61* (11), No. e202109941.
(36) Zheng, N.; Xu, Y.; Zhao, Q.; Xie, T. Dynamic Covalent Polymer Networks: A Molecular Platform for Designing Functions beyond Chemical Recycling and Self-Healing. *Chem. Rev.* **2021**, *121* (3), 1716−1745.
(37) Yang, B.; Miao, W.; Feng, H.; Zhao, Q.; Xie, T.; Zheng, N. On-demand Catalyst-regulated Distinctive Topological Transformations in a Dynamic Covalent Network. *J. Mater. Chem. A* **2022**, *10* (38), 20242−20247.
(38) Miao, W.; Zou, W.; Jin, B.; Ni, C.; Zheng, N.; Zhao, Q.; Xie, T. On demand Shape Memory Polymer via Light Regulated Topological Defects in a Dynamic Covalent Network. *Nat. Commun.* **2020**, *11* (1), 4257.
(39) Wang, S.; Yang, L.; Wang, H.; Xue, L.; Chen, J.; Cui, J. Nonequilibrium Transesterification for Programming a Material's Stiffening. *ACS Appl. Polym. Mater.* **2019**, *1* (12), 3227−3232.
(40) Su, G.; Zhang, Y.; Zhang, X.; Feng, J.; Cao, J.; Zhang, X.; Zhou, T. Soft yet Tough: a Mechanically and Functionally Tissue-like Organohydrogel for Sensitive Soft Electronics. *Chem. Mater.* **2022**, *34* (3), 1392−1402.
(41) Kabe, R.; Adachi, C. Organic Long Persistent Luminescence. *Nature* **2017**, *550* (7676), 384−387.
(42) Zhang, Y.; Su, Y.; Wu, H.; Wang, Z.; Wang, C.; Zheng, Y.; Zheng, X.; Gao, L.; Zhou, Q.; Yang, Y.; Chen, X.; Yang, C.; Zhao, Y. Large-Area, Flexible, Transparent, and Long-Lived Polymer-Based Phosphorescence Films. *J. Am. Chem. Soc.* **2021**, *143* (34), 13675−13685.
(43) Kalita, K. J.; Mondal, S.; Reddy, C. M.; Vijayaraghavan, R. K. Temperature-Regulated Dual Phosphorescence and Mechanical Strain-Induced Luminescence Modulation in a Plastically Bendable and Twistable Organic Crystal. *Chem. Mater.* **2023**, *35* (2), 709−718.
(44) Li, X.-S.; Wu, Y.; Zhao, Y.; Yu, Z.-Q. Employing Cholesterol Copolymerization Strategy for a Thermally Processable Organic Room-Temperature Phosphorescence Material. *Adv. Opt. Mater.* **2021**, *9* (6), 2001893.
(45) Zhang, Y.; Sun, Q.; Yue, L.; Wang, Y.; Cui, S.; Zhang, H.; Xue, S.; Yang, W. Room Temperature Phosphorescent (RTP) Thermoplastic Elastomers with Dual and Variable RTP Emission, Photo-Patterning Memory Effect, and Dynamic Deformation RTP Response. *Adv. Sci.* **2022**, *9* (5), 2103402.
(46) Louis, M.; Thomas, H.; Gmelch, M.; Fries, F.; Haft, A.; Lindenthal, J.; Reineke, S. Biluminescence Under Ambient Conditions: Water-Soluble Organic Emitter in High-Oxygen-Barrier Polymer. *Adv. Opt. Mater.* **2020**, *8* (16), 2000427.
(47) Zhai, Y.; Li, S.; Li, J.; Liu, S.; James, T. D.; Sessler, J. L.; Chen, Z. Room Temperature Phosphorescence from Natural Wood Activated by External Chloride Anion Treatment. *Nat. Commun.* **2023**, *14* (1), 2614.
(48) Somers, P.; Münchinger, A.; Maruo, S.; Moser, C.; Xu, X.; Wegener, M. The physics of 3D printing with light. *Nat. Rev. Phys.* **2024**, *6*, 99.